Structural Engineering and Mechanics, Vol. 14, No. 3 (2002) 287-306
DOI: http://dx.doi.org/10.12989/sem.2002.14.3.287

Seismic assessment of transfer plate high rise buildings

R.K.L. Su†, A.M. Chandler‡ and J.H. Li‡†

Department of Civil Engineering, The University of Hong Kong, Pokfulam Road, Hong Kong SAR, China

N.T.K. Lam‡‡

Department of Civil & Environmental Engineering, The University of Melbourne, Parkville, Victoria 3052, Australia

(Received August 14, 2001, Accepted July 11, 2002)

Abstract. The assessment of structural performance of transfer structures under potential seismic actions is presented. Various seismic assessment methodologies are used, with particular emphasis on the accurate modelling of the higher mode effects and the potential development of a soft storey effect in the mega-columns below the transfer plate (TP) level. Those methods include response spectrum analysis (RSA), manual calculation, pushover analysis (POA) and equivalent static load analysis (ESA). The capabilities and limitations of each method are highlighted. The paper aims, firstly, to determine the appropriate seismic assessment methodology for transfer structures using these different approaches, all of which can be undertaken with the resources generally available in a design office. Secondly, the paper highlights and discusses factors influencing the response behaviour of transfer structures, and finally provides a general indication of their seismic vulnerability. The representative Hong Kong building considered in this paper utilises a structural system with coupled shear walls and moment resisting portal-frames, above and below the TP, respectively. By adopting the wind load profile stipulated in the Code of Practice on Wind Effects: Hong Kong-1983, all the structural members are sized and detailed according to the British Standards BS8110 and the current local practices. The seismic displacement demand for the structure, when built on either rock or deep soil sites, was determined in a companion paper. The lateral load-displacement characteristic of the building, determined herein from manual calculation, has indicated that the poor ductility (brittle nature) of the mega-columns, due mainly to the high level of axial pre-compression as found from the analysis, cannot be effectively alleviated solely by increasing the quantity of confinement stirrups. The interstorey drift demands at lower and upper zones caused by seismic actions are found to be substantially higher than those arising from wind loads. The mega-columns supporting the TP and the coupling beams at higher zones are identified to be the most vulnerable components under seismic actions.

Key words: earthquakes; wind; transfer; structure; displacement; seismic; assessment.

---

† Assistant Professor
‡ Professor
‡† PhD Research Student
‡‡ Senior Lecturer

1. Introduction

In Hong Kong, multiple-purpose high-rise buildings of 30 to 50 storeys height are the inevitable trend, in order to fulfill their function in urban development. The upper parts of the buildings are usually employed for residential purposes while the lower parts of the buildings (typically 3 or 4 storeys) are linked with the podium complex and used for shopping centres, restaurants, clubhouses, car parks or depots. Typical examples in Hong Kong include the re-development of Ho Tung Lau KCRC Depot and the comprehensive development of Discovery Park (Buildings Department 1998). For the tower blocks constructed above the transfer plate (TP) level, reinforced concrete coupled shear walls are usually adopted to achieve the dual purposes of providing partitions for different flats or rooms, together with the main vertical and lateral supports to the upper part of the structure. For the lower parts of such buildings, column-beam frames with or without corewalls are preferred to provide larger clear spaces, column and wall-free areas for different functional uses. Because of the different architectural requirements, transfer structures usually in the form of transfer plates or transfer girders are introduced between the upper and lower zones. The typical thickness of such transfer structures ranges from 2.0 to 3.0 metres and the typical sofit level of the plates are 20 m to 30 m above ground. However, it is well known by seismic engineers (Scott *et al*. 1994) that under cyclic earthquake loads, concentrated stresses and large lateral displacements (termed soft storeys) may occur at a location where there is an abrupt change in stiffness. The potentially flexible frame system below the transfer structure is therefore suspected to be more vulnerable during an earthquake. For this situation, seismic codes often require the use of more elaborate methods of dynamic analysis together with more stringent detailing requirements for the transfer structures, to ensure that the high levels of drift and ductility demand are sustainable without major damage or collapse.

Empirical elastic and inelastic studies of simplified, regular buildings in Hong Kong subjected to earthquake-induced actions were carried out by Pun (1994) and by Chan *et al.* (1998a and 1998b), using a conventional force-based (FB) approach. Both studies compared seismic loads with wind loads for high-rise buildings. They concluded that wind load in Hong Kong is generally more critical than seismic load for high-rise buildings, whilst seismic load (for long return period earthquakes) is more critical for low-rise and mid-rise buildings. It should be recognized that these evaluation studies assumed a constant 'R' factor (the ductility reduction factor or structural response factor) in buildings, regardless of their actual response behaviour and ductility capacity. Thus, the conclusion from such studies would not account for the behaviour of irregular buildings such as one supported by a TP. There are further limitations in these comparative studies. For example, the low to medium-rise buildings located on soft soil sites are additionally vulnerable in the inelastic state and hence require a lower R-factor. It is considered inappropriate to assess the seismic performance of structures assuming an R-factor based on the broad structural classification of the building since the R-factor is often the point of contention. The seismic assessment should specifically address the structure's displacement (or ductility) capacity, which is then compared with the seismic demand.

The aims of this paper are to (i) determine the appropriate seismic assessment methodology for transfer structures using different approaches which can be undertaken with the resources generally available in a design office, (ii) highlight and discuss factors influencing the response behaviour of transfer structures, and (iii) provide a general indication of their seismic vulnerability.

In the present study, various seismic assessment analyses, including response spectrum analysis (RSA), manual calculation, pushover analysis (POA) and equivalent static load analysis (ESA), for

the idealised transfer structures in Hong Kong have been carried out, with particular emphasis on the accurate modelling of higher mode effects and the potential development of the soft storey effect. In conducting this displacement-based (DB) assessment, the corresponding seismic displacement demands for the structure (built either on rock or deep soil sites) were determined from the results of a companion paper (Chandler *et al.* 2000). The lateral displacement demand profile of the building subjected to seismic excitation based on RSA is calculated and compared with the displacement capacity determined by hand calculation. The deformations induced by seismic action are also compared with those from the lateral wind load analysis in Hong Kong. The most vulnerable regions of the structure are thereby identified. For completeness, the load-displacement capacity curves from POA of the building are also determined, despite the fact that representative load patterns are difficult to prescribe and the higher mode effects are difficult to address using this method. Some brief assessment of seismic performance is made, using a direct DB approach (Priestley and Kowalsky 2000).

2. Structural details of the 35 storey transfer plate building

A hypothetical but realistic 35-storey reinforced concrete (RC) tower structure model has been developed, based on Hong Kong design practice. The building is 112.5 m in height, with plan dimensions of 18 m by 56 m, and is supported on a 2.5 m thick transfer plate (TP) at the 6th storey level, which is 20 m above ground as shown in Fig. 1. The tower structure above the TP level is

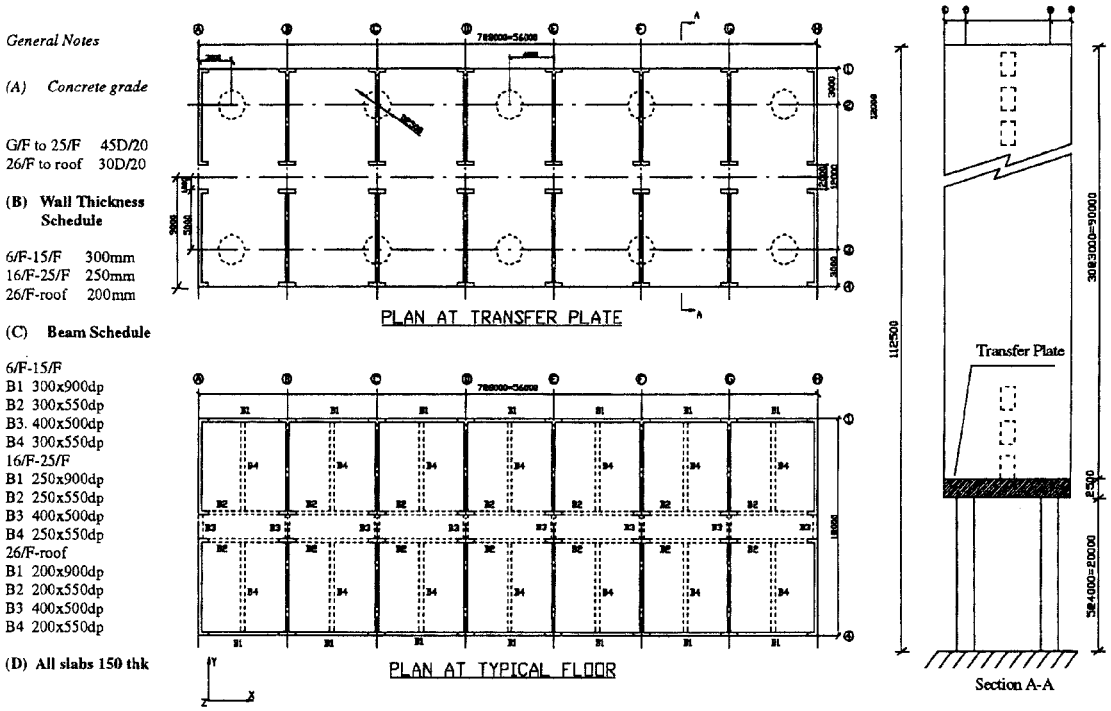

Fig. 1 Example transfer building

Table 1 Design wind load design parameters summary

Storeys	Design Wind Pressure q_i (kPa)
35/F-31/F	3.5
30/F-15/F	3.0
14/F-8/F	2.5
7/F-2/F	2.2
1/F-G/F	1.2

Total wind load $F = C_f q_i A_i$ in which A_i is the effective projected area of the part of the building corresponding to q_i, C_f is equal to 1.155.

supported by coupled shear walls, spaced at 8 m centres, to provide lateral resistance in the Y-direction. Coupling beams, of 550 mm in depth, span 2 m across the gap between each pair of shear walls to provide the coupling actions. Both ends of the coupled shear walls are braced by external shear walls in the X-direction, forming a "closed rigid box". The 5-storey high frame structure below the transfer plate is supported on two rows of 2.5 m diameter "mega-columns" which are restrained at ground and TP level, with vertical span of 20 m.

The building has been designed for floor dead load and live load intensities of 15 kPa and 2.5 kPa, respectively, and these correspond to total unfactored gravitational loads of 533 MN and 80 MN. The design wind load derived in accordance with the Hong Kong Wind Design Code (Buildings Development Department 1983) for a 50-year return period resulted in a design base shear of 19 MN in the Y-direction. Based on the concrete properties specified in the Hong Kong Structural Use of Concrete Code (Buildings Authority Hong Kong 1987), the lateral displacement at roof level in the Y-direction is found to be 165 mm (giving an overall roof drift ratio = 1/677, within the required limiting ratio of 1/500). The design wind pressure for the building is shown in Table 1. It is found that ultimate axial load, bending moment and shear stress of 114 MN ($P/A_g f_c' \sim 0.62$), 35.6 MN-m and 0.6 MPa, respectively, are the resulting actions on the mega-columns. The ultimate gross section shear stress (0.6 MPa) is well below the ultimate shear capacity of 5.0 MPa at supports, indicating that the columns have a very high level of shear capacity.

3. Ductility and drift capacity of mega-columns

3.1 Moment curvature analysis for mega-columns

The RC details of a typical mega-column and wall, based on Hong Kong construction practice (which does not require explicit consideration of seismic actions), are shown in Fig. 2. Each 2.5 m-diameter circular mega-column is reinforced at its lower section by 2 layers of 62 nos. 40 mm diameter high tensile steel reinforcement, which gives a longitudinal reinforcement ratio of approximately 3.2%. The longitudinal reinforcement is then curtailed to equal numbers of 32 mm diameter bars at the upper section.

The lateral concrete confinement of mega-columns in Hong Kong, based on current design practice, is generally very low, as there is no provision for seismic detailing. A typical mega-column is confined with 12 mm diameter circular hoops at a uniform spacing of 300 mm centres, which is

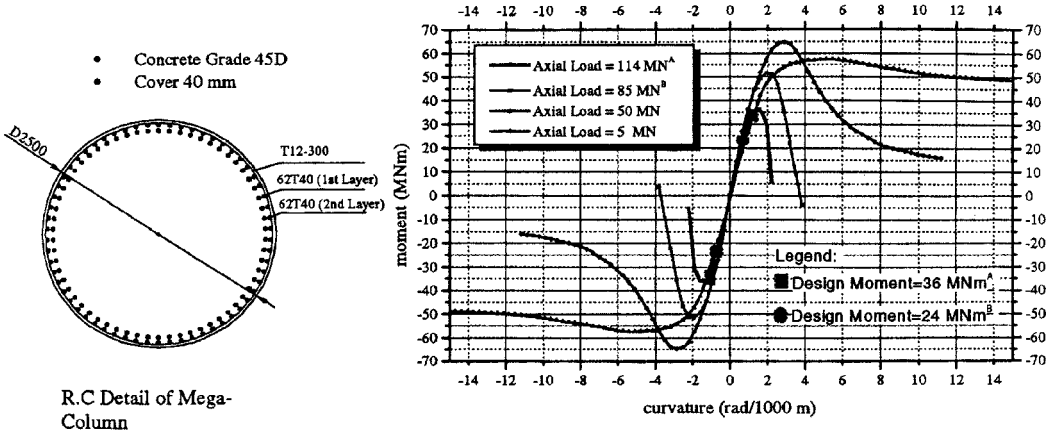

(a) Columns at G/F: 62T40 in 2 Layers

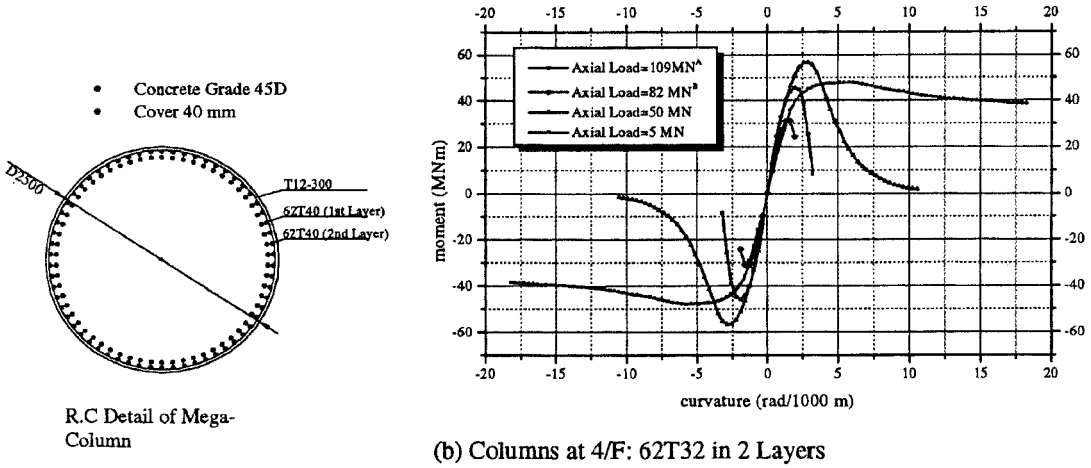

(b) Columns at 4/F: 62T32 in 2 Layers

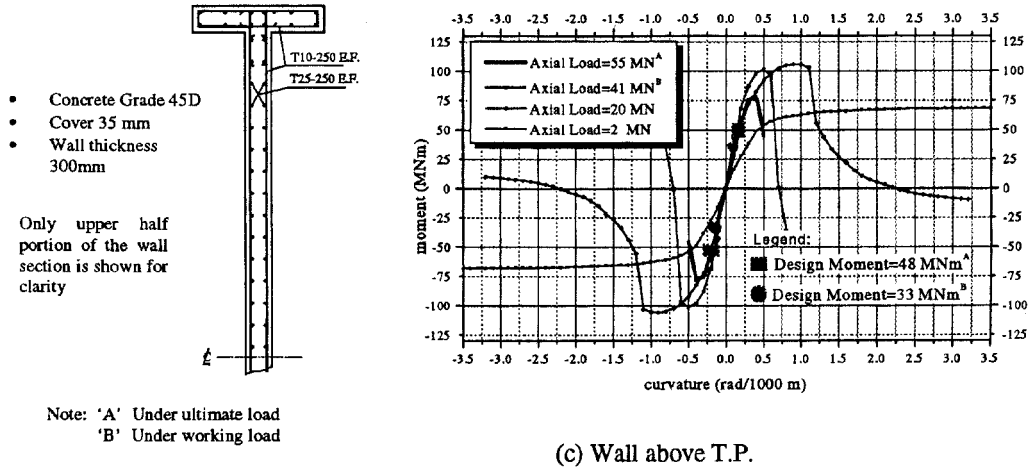

(c) Wall above T.P.

Fig. 2 Moment-curvature relationships

Table 2 Numerical results of the moment-curvature under different axial load conditions

Member	Load Condition	Notional Yield Curvature ϕ_y (rad/1000 m)	Ultimate Yield Curvature ϕ_u (rad/1000 m)	Curvature Ductility Ratio ϕ_u/ϕ_y	Ultimate Moment Capacity (MNm)
Columns at G/F	Ultimate Axial Load (=114MN)	1.17	1.95	1.7	36
	Working Axial Load (=85MN)	1.43	2.48	1.7	52
	Axial Load (=50MN)	1.90	4.31	2.3	65
	Axial Load (=5MN)	2.30	18.2	8.0	57
Columns at 4/F	Ultimate Axial Load (=114MN)	1.10	1.90	1.7	31
	Working Axial Load (=85MN)	1.38	2.64	1.9	46
	Axial Load (=50MN)	1.91	4.25	2.2	57
	Axial Load (=5MN)	2.20	17.6	8.0	48
Shear Walls above TP	Ultimate Axial Load (=114MN)	0.28	0.44	1.6	78
	Working Axial Load (=85MN)	0.34	0.62	1.8	101
	Axial Load (=50MN)	0.50	1.15	2.3	106
	Axial Load (=5MN)	0.40	4.2	10.5	68

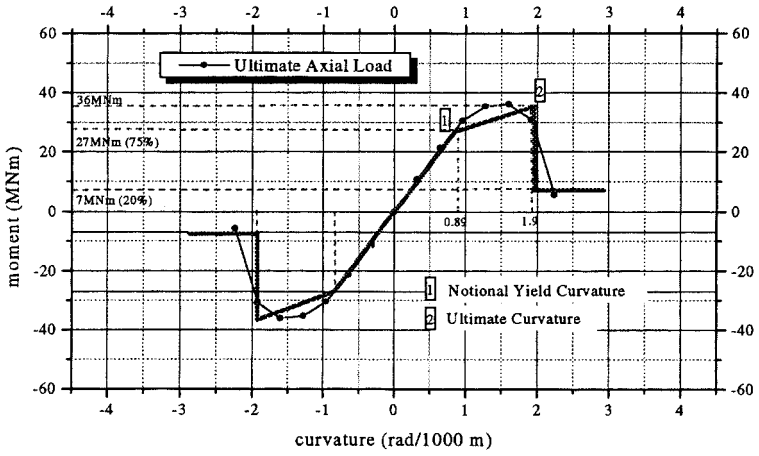

Fig. 3 Idealized moment-curvature relationship at base of mega-columns

equivalent to 0.06% transverse reinforcement volumetric ratio. This detail was adopted in the present analysis. Further, in the presented example, the coupled shear walls possess thicknesses varying between 200 and 300 mm, and include boundary elements to enhance their ductility under lateral loading.

The results of moment-curvature analyses conducted for the mega-columns and a typical wall, as determined by the program RESPONSE (Collins & Mitchell 1997), are shown in Fig. 2, under various axial loading conditions. The ultimate and working design moments of both column and wall are also displayed on the diagrams. The results indicate that at the ultimate loading condition, the mega-column has nearly reached its design ultimate inelastic strength, whilst the wall remains notionally elastic. The mega-columns are therefore likely to be more vulnerable than the shear walls

under environmental lateral loadings. Table 2 summarizes the characteristics of the moment-curvature relationship under different loading conditions. The idealized moment curvature relationship for the columns at ultimate axial loading, utilised for the subsequent POA, is shown in Fig. 3.

3.2 Ductility capacity of the structure by manual checking

Structural analysis of the building, using computer program ETABS (1999), shows that inelastic behaviour (plastic hinge regions) develops first at the bottom and then at the top supports of the column, where bending moments are expected to exceed the yield capacity. The potential "column" collapse mechanism at the bottom part of the building below the transfer plate, as shown schematically in Fig. 4, indicates non-ductile behavior. Thus, the overall displacement ductility capacity of the building (μ_Δ) is derived from the plastic rotational capacity (θ_p) of the column plastic hinges. The value of θ_p is in turn proportional to the dependable ultimate curvature (ϕ_u) of the critical cross-section of the column.

The moment-curvature analysis carried out for the columns using the program RESPONSE (Collins and Mitchell 1997) indicates that the neutral axis is located very close to the extreme tension fibre at the potential plastic hinge locations. Consequently, both the "yield" and "ultimate" conditions are dictated by the limiting compressive strains in the concrete, as shown in Fig. 5. The loading curve for ultimate axial load (Fig. 3) indicates notional yield and ultimate curvatures to be in the order of 1 and 2 radians per 1000 m, respectively. These figures correspond to extremely low curvature ductility capacity (μ_ϕ) of less than 2, which is consistent with the results of Waekava and Xu (2000) who indicated that the ductility of RC columns tends to decrease to a very low level when higher axial compressive force is applied. A slightly improved strength and ductility performance has been shown with a co-existing working axial load. It is useful to note that the rare event of a severe earthquake is unlikely to co-exist with a rare gravitational overload. Comparisons with other axial load conditions are shown in Fig. 2. However, the seismic overturning moment of

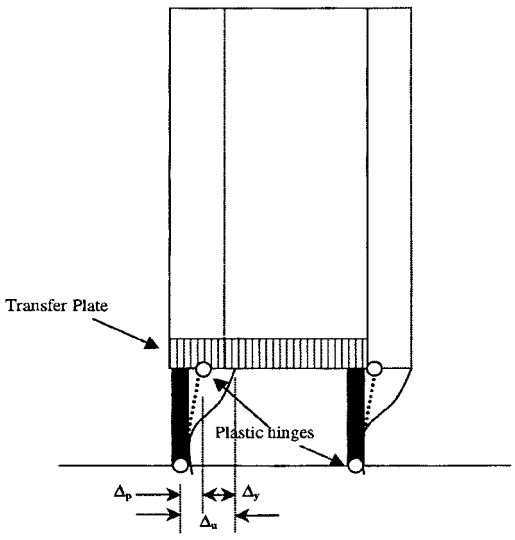

Fig. 4 Schematic diagram showing failure mechanism of mega-columns supporting transfer plate

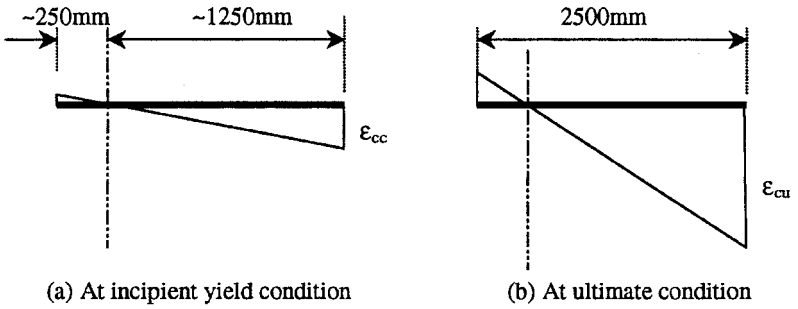

Fig. 5 Schematic column strain diagrams

the building is expected to significantly increase the dynamic axial load associated with the push-pull action of the columns. Thus, the conservative approach of assuming ultimate axial load has been adopted in the ductility capacity assessment described below.

A manual checking procedure has been undertaken to assess the limiting curvatures in the columns at different stages of loading. At ultimate condition, the curvature of the critical cross-section in the column can be determined in accordance with the depth of the neutral axis and the dependable ultimate compression strain (ε_{cu}) of concrete, based on the following expression (Priestley 1996, Priestley & Calvi 1997, Kowalsky *et al*. 1995):

$$\varepsilon_{cu} = 0.004 + 1.4\ (\rho_{sh} f_{yh} \varepsilon_{shu} / f'_{cc}) \tag{1}$$

where :

f_{yh} = yield strength of the hoop reinforcement (460 MPa)
ε_{shu} = limiting tensile strain of the hoop reinforcement at the maximum stress condition (= 0.06)
f'_{cc} = maximum compressive strength of the confined concrete (~$1.5 f'_c$ or 1.5 × 37.45 MPa = 56 MPa)
ρ_{sh} = volumetric ratio of the hoop reinforcement = $4\ A_{bh}/s\ D_c$
A_{bh} = area of a single 12 mm diameter hoop bar (113 mm^2)
s = spacing of the hoop reinforcement (300 mm)
D_c = diameter of the confined concrete (area enclosed by the circular hoop) ~ 2.5 m (D) (2)

Eqs. (1) & (2) provide an estimate of ε_{cu} as 0.0044, which is not significantly greater than the threshold value of 0.004 for unconfined concrete. Thus, the hoop reinforcement provides a very low level of confinement, which results in a negligible enhancement in the ductility of the plastic hinge. Given that the neutral axis is positioned at 2250 mm from the extreme compression fiber (0.9D), due to the high level of pre-compression (Fig. 5b), the ultimate curvature (ϕ_u) is accordingly equal to 0.0044/(0.9 × 2.5 m), or 2.0 radian/1000 m (or 0.002 radian/m). This figure is in close agreement with Fig. 2b results.

The incipient yield curvature (when first yielding occurs) at the plastic hinge (ϕ'_y) is expected to be associated with the compressive yielding of concrete, as opposed to the compressive yielding of the reinforcement, due to the high pre-compression axial loads. The incipient yield curvature may be expressed as:

$$\phi'_y = \varepsilon_{cc}/(0.9D) \tag{3}$$

where :

ε_{cc} = incipient yield strain of concrete = f'_c/E_c (4)

f'_c = characteristic compressive strength = 37.45 MPa

E_c = tangential Young's modulus ~ $500\sqrt{(f'_c)}$ = 30600 MPa (Mander *et al.* 1988) (5)

Eqs. (4) & (5) give $\varepsilon_{cc} = 0.0012$, which is then translated to $\phi'_y = 0.0012/(0.9 \times 2.5\text{ m}) = 0.53$ radian/1000 m according to Eq. (3). For circular cross-sections in particular, the initial yielding of the reinforcement (located furthest away from the neutral axis) occurs at a curvature well below that of overall yielding of the entire cross-section, the latter indicating the formation of the plastic hinge mechanism. It is estimated that the notional yield curvature (ϕ_y) is in the order of twice the incipient yield curvature (ϕ'_y) (Priestley 1998). Thus, ϕ_y is taken to be approximately 1.06 radian/1000 m. As a matter of interest, the strain at which the reinforcement yields is 0.0019, which corresponds to a curvature of 0.85 radian/1000 m, just less than the notional yield curvature value given above.

Note that the above assessment implies an extremely low curvature ductility capacity of less than 2 (i.e., 2.0/1.06). An alternative procedure to determine curvature ductility based on research in New Zealand can be found in Watson *et al*. (1994) which was based on the original work of Mander *et al*. (1988). However, a much higher curvature ductility ratio of 8 was obtained. The discrepancies highlight the need to exercise caution when applying empirical relationships, which can be based on very different parameter ranges and assumptions.

The plastic rotational capacity (θ_p) of the column plastic hinge can be obtained using the expression:

$$\theta_p = (\phi_u - \phi_y)\, L_p \tag{6}$$

where :

Plastic hinge length (m) (L_p) = $0.08\, L + (f_y/270)\, 6\, d_{bl}$ (Priestley 1996) (7)

L = length measured to the point of contraflexure which is assumed to be half column height (10 m)

f_y = 460 MPa

d_{bl} = diameter of longitudinal reinforcement = 40 mm

It should be noted that the significant effect of yield penetration has been accounted for by the second term in Eq. (7). Eqs. (6) & (7) estimate L_p at approximately 1.1 m and hence $\theta_p = (0.002 - 0.00106) \times 1.15 = 0.0011$ radian. Thus, the plastic displacement or column drift capacity (Δ_p) according to Fig. 4 is:

$$\Delta_p = \theta_p \times L = 0.0011 \times 20000\text{ mm} = 22\text{ mm} \tag{8}$$

The lower bound yield displacement or drift (Δ_y) associated with the mega-columns displacing with fixed supports at both ends is conservatively determined from the following simplified expression (Calvi and Pavese 1995):

$$\Delta_y = \phi_y H^2/6 = 0.00106 \times 20^2/6 \times 10^3 = 71\text{ mm} \tag{9}$$

Note that the expression of Eq. (9) assumes that the connection of the top of the column with the TP is relatively rigid, which is appropriate in this instance.

The sum of the limiting plastic displacement [Eq. (8)] and yield displacement [Eq. (9)] predicted at the top of the mega-columns according to the above calculations is 93 mm (giving the ultimate column drift capacity, Δ_u). The drift ductility capacity (Δ_u/Δ_y) below the transfer structure is accordingly 93/71 = 1.3, which is considered negligible. This aspect is analysed and further discussed below.

A follow-up investigation leads to the interesting finding that there is only a moderate increase in

the drift ductility capacity of the column, even if the spacing of the confining hoop reinforcement has been reduced from 300 mm down to 50 mm (i.e., a six fold increase in the quantity of the reinforcement). It can be shown that ε_{cu} is thereby increased from 0.0044 to 0.0058 [Eq. (1)], and ϕ_u is correspondingly increased from 0.0020 to 0.0026. The resulting increase in Δ_p is from 22 mm to 54 mm [Eqs. (6) & (8)], which is translated to an increase of the drift ductility capacity from 1.3 to around 1.7. Thus, the adoption of "good detailing" alone is neither always effective nor adequate in improving the potential seismic performance behaviour of the mega-columns, and hence the building as a whole. Calculation also shows that, for the column specimen selected in the present study, around ten times (0.6%/0.06%) larger transverse reinforcement volumetric ratio is demanded in order to meet the increase of the drift ductility capacity from 1.3 to 2.0. However, such measures are difficult to carry out in practice (for the considered column specimen), in order to increase the transverse reinforcement volumetric ratio to 0.6% or greater. It is noted that, even then, the resulting displacement ductility capacity remains relatively low. To effectively retrofit a building for improving its potential seismic performance, the underlying physical processes governing its capacity to resist lateral loadings must be correctly addressed. It is clear from the foregoing analysis that the position of the neutral axis associated with the high level of axial pre-compression is the main contributor to the potentially non-ductile behaviour of the columns, and that this high pre-compression level cannot be easily eliminated as it is an integral feature of the Transfer Structure and its design.

The overall displacement ductility capacity of the building can be even smaller than the drift ductility of the columns, due to the elastic deflection of the upper section of the building above the TP level. As this elastic displacement reserved at the upper part of the building does not undergo inelastic deformation, seismic energy absorbed in the building cannot be effectively dissipated at that part of the structure.

4. Ductility and drift demand of the building

4.1 Modified stiffness for the building

It is not straightforward to determine the actual stiffness of reinforce concrete as it depends on a number of factors including dynamic stiffening, aging, steel ratio and extent of cracking in concrete under tensile loads. Typical elastic modulus of concrete can be determined either from codes of practice or from uni-axial compressive tests. The effects of transient load application and aging may increase the modulus by approximately 40% and 10%, respectively (Lee *et al*. 2000 and BSI 1985). In addition, the flexural stiffness of a concrete element could depend significantly on the reinforcement content. It was pointed out by Priestley (1998) and by Priestley and Kowalsky (1998) that the section stiffness may not be considered as a fundamental section property. The stiffness of the section would be altered by changes in axial load ratio or flexural reinforcement content, due to the non-linear behaviour of the reinforced concrete and the variation of the effective sectional area for cracked sections. The stiffnesses of vertical members have therefore been modified herein, under ultimate conditions, with the factors applied to the stiffnesses of column, beam, and wall being 0.8, 0.5 and 0.75, respectively. These factors were derived according to design values presented in the above references, modified appropriately to allow for the relatively low levels of seismic displacement demand, as discussed in the following paragraphs. To take into account all the above contributions, the elastic modulus of the RC structural members has been increased by 30 to 40%

Table 3 Modal parameters

Mode number	Period (sec)	Accumulative effective mass factors (%)	Percentage of effective mass factors (%)
1	3.08	72.4	72.4
2	1.00	95.2	22.8
3	0.42	96.4	1.2
4	0.22	96.6	0.2
5	0.13	96.8	0.2

when compared with the values stipulated in the design code (Building Authority 1988).

By using the structural model with modified stiffness, free vibration analysis was carried out. The vibration periods and cumulative effective mass factors in the Y-direction, for the first 5 modes, are shown in Table 3. It is noted that the fundamental vibration period of the building is 3.08 sec. The effective mass factors for the first and second modes are equal to 72% and 23%, respectively. The cumulative effective masses for the first and second modes contribute to 95% of the total cumulative effective mass. Thus, the results indicate that the second mode effects (or higher mode effects) are likely to be significant.

4.2 Response Spectrum Analysis (RSA)

The displacement demand on a SDOF structure is simply the spectral displacement (at the initial period, assuming 5% damping). However, it is important to point out that the displacement spectrum must account for the potential effects of soil resonance, which is very sensitive to the depth of the soil sediments and the impedance contrast between the soil and bedrock. Such effects can be estimated by the non-linear wave analysis of the soil column [for example, using computer program SHAKE (Idriss and Sun 1992)] or alternatively by a new and simple manual procedure known as FASA (Lam *et al.* 2001 and Sheikh 2001). Existing empirical response spectrum models which do not explicitly parameterise sediment depths might not have fully accounted for the soil resonance effect, which is particularly detrimental to non-ductile structures (including transfer structures) commonly found in low to moderate seismicity regions.

It is outside the scope of this paper to address seismic hazard modelling or response spectrum modelling in detail. Nevertheless, a rock and a soil acceleration and displacement response spectrum estimated for a 2500-year return period far-field event affecting Hong Kong are shown in Figs. 6a and 6b, respectively, for purposes of illustration. The stochastically-simulated bedrock earthquake records are generated by the program GENQKE (Lam *et al*. 2000a) such that the ensemble average spectrum closely matches the target response spectrum (Fig. 6a). The background to the development of the target response spectrum of the rock site is described in Lam *et al.* (2000b and 2000c). Detailed geotechnical information for the soil site can be referred to Site A of GEO(1997). It is shown in Fig. 6b that RSD(T_i = 3.08 sec) = 24 mm and 50 mm, for the rock and soil sites, respectively.

The displacement spectrum at a notional 5% critical damping is normally provided from seismic hazard studies. Thus, a reduction factor is often used to allow for hysteretic energy absorption arising from the inelastic excursion of the structure to the ultimate condition. This adjustment factor can be based on artificially increasing the viscous damping to emulate hysteretic energy absorption (Priestley 1996). Alternatively, empirical inelastic response spectra have also been used in deriving

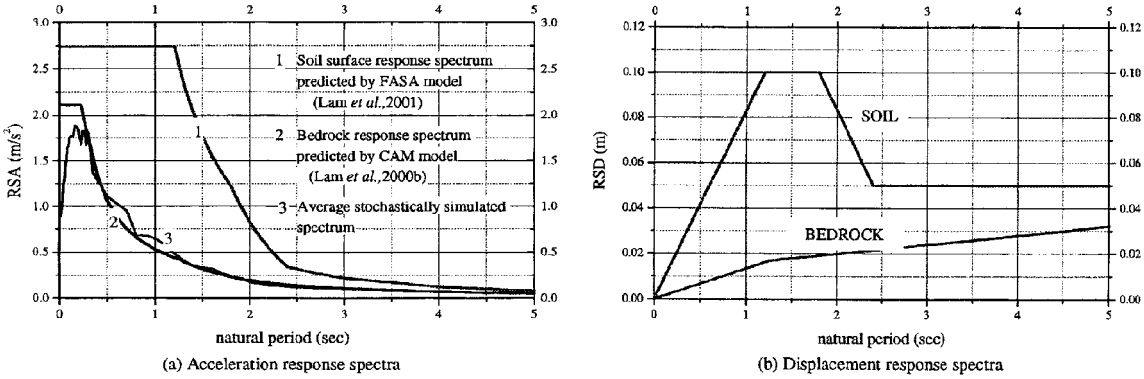

Fig. 6 Proposed idealised response spectra for rock and soil sites (accounting for soil resonance) (after Lam *et al.* 2000b, 2001, Sheikh 2001)

suitable adjustment factors to account for inelastic behaviour (Chopra and Goel 1999). However, it was shown earlier in the paper that the capacity of the transfer plate (TP) structure to respond in the inelastic range is very limited. Thus, the hysteretic energy absorption associated with the inelastic response is expected to be very small. Nevertheless, non-linear behaviour such as cracking of reinforced concrete would result in some hysteretic energy absorption within the notional yield limit. In addition, there may be certain energy dissipation by the non-structural components. A generalised analytical solution to damping of this nature is difficult to develop, due to the variability between buildings and the lack of information on the non-structural components. Thus, further research is warranted to quantify the contributions of energy absorption by various structural and non-structural components in the building, such that damping can be determined in a rational manner. In the interim, reference is made to Newmark and Hall (1982), who considered that concrete structures generally respond with 5-10% critical damping "at or just below the yield point". Since only localized damage is expected to happen at the supports of the non-ductile mega-columns and partial damage to non-structural components, damping ratio of 5% is recommended as the overall (lumped) allowance for hysteretic energy absorption in the building.

By using the modified stiffness model and 5% damping, a detailed response spectrum analysis (RSA) was implemented by using the computer package ETABS (1999). High-rise buildings are expected to behave elastically under low to moderate seismic actions. The elastic seismic displacement demand profiles determined by RSA are shown in Fig. 7. We found that at the building's effective height, taken according to Priestley (1996) as 0.65 *h*, the displacement demands determined by RSA (with the first two response modes considered) are 23 mm and 48 mm for rock and soil sites, respectively. These values are closely matched with RSD(T_i) from the equivalent SDOF system, quoted above. For each site condition, two displacement profiles are shown in Fig. 7 corresponding to the effects caused by the first vibration mode only and the combined effects from analyzing the first two modes or more. The maximum discrepancy between the two profiles is as high as 470%, which is associated with the case of soil site at transfer plate level. The reason for such a large discrepancy is due to the fact that the second vibration mode possesses a relatively large effective mass factor (23%, Table 3) and furthermore that the vibration period of 1.0 sec falls into the range of maximum displacement response on the soil response spectrum curve as shown in Fig. 6b. Thus a high displacement demand at TP level is generated from the contribution of the second vibration mode.

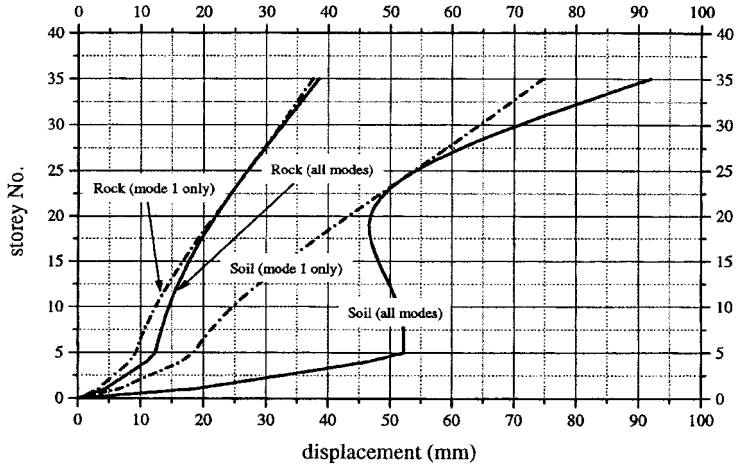

Fig. 7 Displacement profiles from dynamic response spectrum analysis (RSA)

The comparison of RSA displacement profiles in Fig. 7, especially for the soil site, strongly indicates that the lateral displacement demand of the building is significantly affected by the higher mode contributions, especially that arising from mode 2. The influence of higher modes on displacement demands is particularly evident at the roof (h) and TP levels of the building, but interestingly is less important when considering the displacement at effective height (0.65 h). This implies the important result that simply obtaining a prediction of displacement demand at effective height level, using an equivalent SDOF system approach, does not necessarily result in an accurate estimation of displacements for the building as a whole.

The maximum predicted displacement demand at the TP level (52 mm, for the soil site) is noted to be smaller than the estimated yield displacement from earlier analyses, namely 71 mm. This result supports the decision to conduct elastic RSA analysis as the most appropriate method for determining the seismic displacement demands.

The average lateral drift ratio of the building (defined as the ratio of roof displacement to the total building height) has been computed using the RSA analyses as 1/2860 and 1/1170, for rock and soil sites, respectively. The maximum inter-storey drift ratios θ_{1max} (ratio of interstorey drift displacement to storey height) associated with the first mode of the building are 1/2100 and 1/860, respectively, for rock and soil sites. However, despite these relatively low values of average lateral drift ratio, it is important to ascertain also what are the maximum values of interstorey drift ratio for combining all the vibration modes. This is because of the widespread recognition that maximum interstorey drift ratio better reflects the onset of nonstructural component damage, as well as potential structural damage (Priestley 1996). The maximum interstorey drift ratios θ_{max} of the building, founded on rock and soil sites, are shown in Fig. 8. The results are compared directly with the interstorey drift demands from static wind loading. It is shown that the maximum seismic interstorey drift ratios occur between foundation and TP level, and have values of 1/1630 and 1/380, for rock and soil sites, respectively. These interstorey drift ratios are significantly higher than the corresponding lateral drift ratios θ_{1max} given above, by a factor ($\theta_{max}/\theta_{1max}$) of 1.3 for the rock site and 2.3 for the soil site. These factors have been termed higher mode drift factors (Chandler *et al.* 2002) or dynamic amplification factors [Paulay and Priestley 1992], with recommended values of 1.3-1.8.

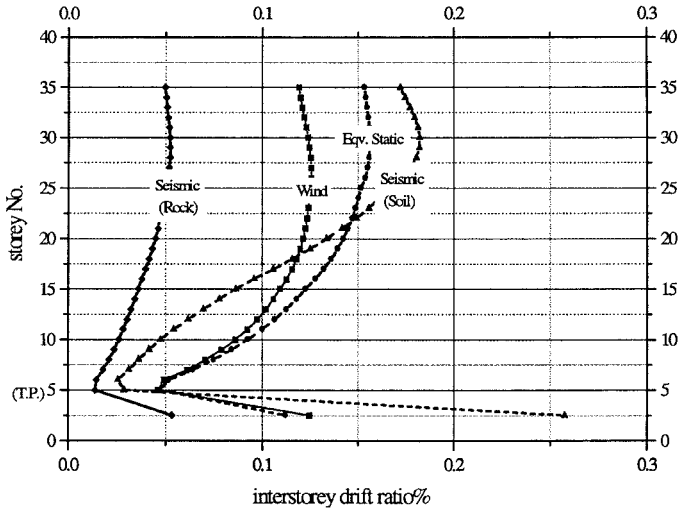

Fig. 8 Interstorey drift ratios

These recommended values are much smaller than the value computed for soil site in the present study, which again clearly emphasizes the importance of soil site amplification and higher mode contributions to the dynamic response of high-rise TP buildings.

4.3 Comparisons of displacement demand with capacity

The comparison of the maximum interstorey drift demand and capacity over the entire height of the building is an effective way to identify any local distortions and hence any local overloading at particular floors. The RSA reveals that a relatively high seismic interstorey drift demand occurs below the TP level (see Fig. 8). The supporting mega-columns with their inherent brittle nature are therefore expected to be more vulnerable than the other structural components. The maximum lateral displacement demand at TP level as determined in the previous section is 52 mm corresponding to a 2500-year return period, far-field earthquake at the soil site. The ultimate displacement capacity estimated by using manual calculation (see above) is 93 mm. When comparing the seismic displacement demand with capacity, a safety margin of 1.8 can be found. Hence, the building has a low probability of ultimate collapse in the form of a soft storey failure under seismic action in Hong Kong. It is also noted from Fig. 8 that the maximum seismic interstorey drift demands exceed those from wind loading, in the upper levels of the building. This result is further discussed, below.

5. Review of seismic assessment methodologies

5.1 Modal response spectrum analysis

The detailed modal response spectrum analyses (RSA) conducted herein have clearly demonstrated the appropriateness of such a technique for accurately determining the seismic

displacement demands for high rise TP buildings in a low to moderate seismic region. In particular, the RSA is capable of capturing the important contribution to total seismic response that arises from the higher dynamic vibration modes. Such contributions have been shown to increase the maximum interstorey drift demand ratios by a factor of up to 2.3, when compared with the maximum drift ratio $\theta_{1\max}$ of the first mode. Such increases indicate that comparisons of seismic demands with wind demands, based purely on considerations of maximum base shear, cannot adequately account for the dynamic displacement demands arising from seismic actions.

5.2 Pushover Analysis (POA)

As an alternative to manual calculation, the displacement capacity of the building structure as a whole may be obtained by static POA (Calvi and Pavese 1995, Park 1996, Krawinkler and Seneviratna 1998, Mwafy and Elnashai 2001), which takes into account both the column drift and the deflection of the structural walls supporting the building tower above the TP. POA is a simple tool for evaluating the behaviour of structures responding into the inelastic range under lateral loading. Essentially, a lumped mass single-degree-of-freedom (SDOF) system is created and under lateral loading the correct ratio of its mass and initial stiffness is determined such that initial natural period of vibration matches the fundamental natural period of vibration of the original multi-degree-of-freedom (MDOF) model. The initial natural period matching will automatically result in the response displacement time-histories at any point on the MDOF structure which are proportional to that of the SDOF model, provided that the response is dominated by a single fundamental mode. Krawinkler and Seneviratna (1998) highlighted the fact that the deflection profiles obtained by POA and by dynamic analysis are closely correlated for low-rise structures but can differ significantly for tall buildings in which higher mode effects become important. The linear and nonlinear behaviours are sensitive to the chosen pattern of lateral load. The load patterns adopted may not give good estimates of dynamic interstorey drift ratios over the entire height, since different load patterns may induce different localized mechanisms in a structure, and furthermore it will depend on the frequency characteristics of the ground motion which, if any, of these localised mechanisms will be activated and amplified in an earthquake. Bearing in mind the above considerations, it is herein recommended that three load patterns are selected for carrying out such POA. The first loading pattern is determined by iteration such that its shape is proportional to the deflection shape of the building throughout the elastic range of response. The second load pattern attempts to capture the soft storey effect and provides an essentially constant loading above the TP level, being linearly decreased to zero from TP to ground level. The third load pattern attempts to capture the higher mode effects and is proportional to the SRSS combination interstorey shear obtained from RSA. These three load patterns are illustrated in Fig. 9.

Program ETABS (1999), in which account is also taken of P-delta (secondary moment) effects, has been used herein to accomplish the procedures of POA described above. The ultimate displacement capacities (δ_u) at the effective height have been calculated and the resulting lateral capacity curves are shown in Fig. 9. The ultimate roof displacements, which are sensitive to different load patterns, range from 230 mm to 295 mm. The third load pattern (proportional to the interstorey shear from RSA) gives the smallest ultimate displacement capacity, associated with the most conservative results. Small deviations (less than 10%) of the ultimate base shear are observed when different load patterns are applied. The displacement profiles at notional yield limit and ultimate limit are shown in Fig. 10. Despite the fact that the consistent ultimate displacement

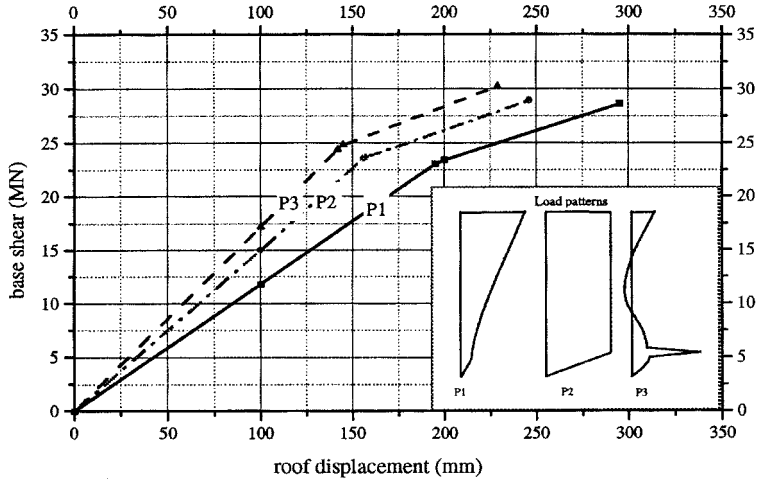

Fig. 9 Lateral capacity of the building from POA

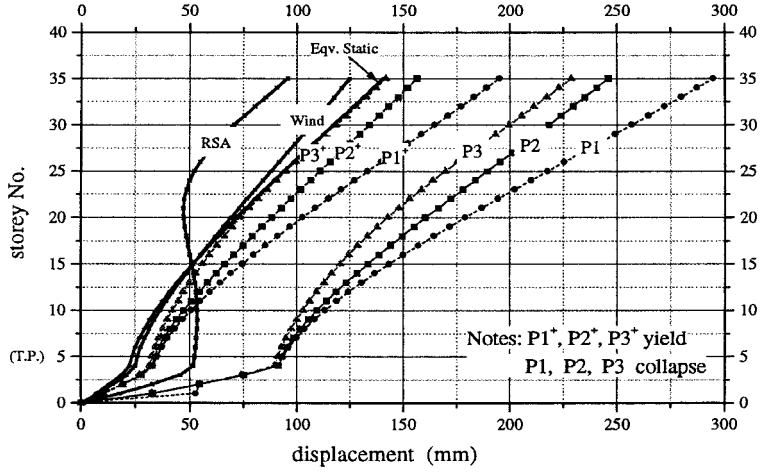

Fig. 10 Lateral displacement capacity of the building from POA

capacities below TP level of 91 mm are calculated, clear differences in the displacement profiles are observed when adopting different lateral load patterns. However, none of the displacement shapes is similar to that calculated by using RSA, which is considered to be more accurate in the elastic range of response. The result once again demonstrates that POA does not give accurate results when higher mode effects are significant. It is noted that the ultimate displacement capacity for the mega-column, as predicted by hand calculation (93 mm) is in close agreement with the value (91 mm) obtained from POA. In a DB assessment, the ultimate displacement capacity of the building is usually compared with the seismic displacement demand at the effective height taken as 0.65 *h* of the building, (Priestley 1996). In comparison with the building's ultimate displacement capacity, it is observed that the 2500-year return period earthquake demand on the soil site (48 mm at effective height) is, as expected, lower than the capacity (153 mm, load pattern 3) by a factor of ~3.2. This

factor of safety is much higher than that determined using RSA (1.8) and may be regarded as being artificially conservative since the POA has not captured the important higher mode contributions.

5.3 Comparison of seismic and wind demands

By using the modified stiffness model, the displacement demand profile arising from wind loading is calculated and presented in Fig. 10. It can clearly be seen that at both roof and effective height level, the displacement demand predicted by wind load is higher than that of the seismic actions (soil site). However, it should not be simply concluded that the demand for seismic actions is less than that of wind. As mentioned previously, the interstorey drift ratio associated with local deformations usually gives a better indication on the local member demands. Fig. 8 compares the interstorey drift ratios of wind and earthquake at soil and rock sites. It is found that at regions below TP and higher than 18/F, seismic demands are, in fact more critical than wind demands. The results imply that not only are the mega-columns critical, but also the shear walls and especially the coupling beams at a higher zone are also critical and could be damaged under seismic actions.

5.4 Equivalent Static Lateral Load Analysis (ESA)

Following the procedure described in the code UBC (1997), ESA for the building was carried out. To take into account the stiffness contributions from the non-structural components, the fundamental period of structure is decreased by 20% (Mayes 1995) and gives T_n = 2.57 sec. The period is found to be consistent with that estimated from the empirical formula of frame structures given in the UBC code (T_n = 0.0731 $h^{3/4}$, h = 112.5 m) which predicts T_n = 2.53 sec. The modal mass M_e (= 52100 tonnes) of the building is assumed to be 85% of the actual mass of the building. Referring to Fig. 6a, the spectral acceleration RSA for soil site at period T_n is found to be 0.32 m/s^2. The base shear determined by the formula $V = M_e \times RSA$ is equal to 16.7 MN. The distribution of the equivalent static lateral shear at each floor can be accomplished by the expressions:

$$V = F_t + \sum_{i=1}^{n} F_i \tag{10}$$

$$F_t = 0.07\ T_n V \le 0.25 V \tag{11}$$

$$F_i = (V - F_t)\frac{w_i h_i}{\sum_{i=1}^{n} w_i h_i} \tag{12}$$

where F_t is the shear force applied at the roof (in this case, equal to 0.18 V), n is the total number of stories, w_i is the weight at a particular level and h_i is the height of a particular level above the base. At each floor, the force F_i is located at the mass centre.

The lateral displacement demand profile by the ESA is shown in Fig. 10. Although the seismic base shear (16.7 MN) is less than that of wind (19 MN), the induced roof displacement (140 mm) by earthquake is greater than wind (124 mm) due to a large concentrated load F_t acting at roof in the seismic analysis. The demands on interstorey drift ratio for the ESA, together with RSA, are shown in Fig. 8. It is found that the drift ratio in upper part of the building is less than that from RSA by around 15% while in the lower part of the building above TP, the drift ratio predicted by

the ESA is significantly overestimated by around 65% when compared with the RSA. Furthermore, ESA cannot capture the soft storey effect and underestimates the interstorey drift demands at TP level by 55% when compared with RSA. Finally, the displacement profile (shown in Fig. 10) obtained from the ESA also does not match the same obtained from the RSA. The results clearly reveal that the ESA, as with POA described above, cannot produce reliable results for situations where higher mode effects and soft storey effects are significant.

6. Conclusions

The aims of this paper are to (i) determine the appropriate seismic assessment methodology for transfer structures using different approaches which can be undertaken with the resources generally available in a design office, (ii) highlight and discuss factors influencing the response behaviour of transfer structures, and (iii) provide a general indication of their seismic vulnerability. The main conclusions of this study are as follows:

1. Structural seismic assessments for Transfer Structures in low to moderate seismicity regions require specific account to be taken of the acute lack of ductility arising in mega-columns supporting the transfer plate, which results directly from the high pre-compression axial forces in such columns.
2. The acute lack of ductility of high rise transfer structures, at both member and global levels, indicates that the ratio of ultimate and notional yield displacement capacities is extremely low. The possibility of brittle-type failures of the mega-columns of such structures, under excessive earthquake-induced actions, is therefore a matter of some concern.
3. The addition of more stringent confinement regulations for such columns (such as reducing the maximum spacing of stirrups) may not have a significant effect on the ductility capacity of the structure as a whole. This aspect is considered worthy of further research.
4. The RSA reveals that a substantially high interstorey drift ratio demand is located below the TP level; mega-columns with inherent brittle nature are therefore expected to be more vulnerable than the other structural components.
5. When the results of dynamic multi-mode RSA are compared with simplified and widely used methods such as POA and ESA, it is revealed that accurate estimation of seismic displacement demands in transfer plate high rise buildings can only be achieved by using RSA, which captures the important contributions of the higher vibration modes. Even though POA and other static techniques may give reasonable predictions of the seismic displacement demands at a notional effective height in the building, it is demonstrated that the lateral drift ratio $\theta_{1\max}$ from such analyses can underestimate the maximum seismic interstorey drift ratio by a factor of up to 2.3. This dynamic amplification factor exceeds recommended values (1.3-1.8) by a wide margin.
6. When comparing the seismic displacement demand with ultimate capacity, a safety margin of 1.8 was found. Hence, the example building has a low probability of ultimate collapse in the form of soft storey collapse under the long return period seismic actions in Hong Kong, even when site resonance effects are considered.
7. By comparing the interstorey drift demands of wind load and earthquake load at a typical soil site, it is found that seismic actions are more critical than wind load, at regions below the TP and higher than 18/F. The results indicate that both the mega-columns and the coupling beams at higher zones are critical and could be damaged under seismic actions. The assumption that

tall buildings in Hong Kong and other low to moderate seismic regions experience seismic demands that are much smaller than those considered for wind design purposes, has therefore been proved somewhat questionable.

Acknowledgements

The authors thank The University of Hong Kong for supporting the project by University Research Committee (URC) Research Initiation Grant (2000-2001). The work described in this paper has been funded by the Research Grants Council of Hong Kong, China (Project No.'s HKU 7023/99E and HKU 7002/00E), whose support is gratefully acknowledged. This paper has also been developed as a result of a project funded by the Australian Research Council (large grant), entitled: "Earthquake Design Parameters and Design Methods for Australian Conditions" (AB89701689).

References

British Standards Institution (BSI) (1985), *Code of Practice for Design and Construction* (BS8110 Part 2), *British Standard, Structural Use of Concrete*.

Buildings Authority Hong Kong, HKSAR (1987), Code of Practice for Structural Use of Concrete.

Buildings Department, HKSAR (1998), Building Construction in Hong Kong.

Buildings Development Department (1983), *Code of Practice on Wind Effects : Hong Kong-1983*, Government of Hong Kong, Hong Kong.

Calvi, G.M. and Pavese, A. (1995), Displacement Based Design of Building Structures. *European Seismic Design Practice*, Balkema, Rotterdam, 127-132.

Chan, H.C., Pan, A.D.E., Pam, H.J. and Kwan, A.K.H. (1998a), "Seismic detailing of reinforced concrete buildings with relevance to Hong Kong design practice (Part I)", *Transactions of the Hong Kong Institution of Engineers*, **5**(1), 6-13.

Chan, H.C., Pan, A.D.E., Pam, H.J. and Kwan, A.K.H. (1998b), "Seismic detailing of reinforced concrete buildings with relevance to Hong Kong design practice (Part II)", *Transactions of the Hong Kong Institution of Engineers*, **5**(1), 14-20.

Chandler, A.M., Su, R.K.L., Sheikh, N. and Lam, N.T.K. (2000), "Motion induced by distant earthquakes: effect of sediments and reclamation", *Proc. Int. Conf. Advances in Structural Dynamics (ASD2000)*, The Hong Kong Polytechnic University, **1**, 185-192.

Chandler, A.M. Su, R.K.L. and Lee, P.K.K. (2002), "Seismic drift assessment for Hong Kong Buildings", *Proceedings of the Annual Seminar 2001/02*, The Hong Kong Institution of Engineers Structural Division & The Institution of Structural Engineers (HK Division), 17 May 2002, 1-15.

Chopra, A.K. and Goel, R.K. (1999), "Capacity-spectrum-demand methods based on inelastic design spectrum", *J. Earthquake Spectra*, **15**(4), 637-656.

Collins, M.P. and Mitchell, D. (1997), *Prestressed Concrete Structures*, Response Publications, Canada.

GEO (1997), *Pilot Study of Effects of Soil Amplification of Seismic Ground Motions in Hong Kong, Technical Note TN 5/97*, Geotechnical Engineering Office, Civil Engineering Department, Hong Kong.

ETABS (1997), *Three Dimensional Analysis of Building Systems (version 7.12), User's Manual*, Computers & Structures Inc.

Idriss, I.M. and Sun, J.I. (1992), *User's Manual for SHAKE-91*, sponsored by National Institute of Standards and Technology, Maryland, U.S.A. and Department of Civil & Environmental Engineering, University of California, Davis, U.S.A.

Kowalsky, M.J., Priestley, M.J.N. and MacRae, G.A. (1995), "Displacement-based design of RC bridge columns in seismic regions", *Earthq. Eng. Struct. Dyn.*, **24**, 1623-1643.

Krawinkler, H. and Seneviratna, G.D.P.K. (1998), "Pros and cons of a pushover analysis of seismic performance evaluation", *Eng. Struct.*, **20**(4-6), 452-464.
Lam, N.T.K., Wilson, J.L. and Hutchinson, G.L. (2000a), "Generation of synthetic earthquake accelerograms using seismological modelling: a review", *J. Earthquake Engineering*, **4**(3), 321-354.
Lam, N.T.K., Wilson, J.L., Chandler, A.M. and Hutchinson, G.L. (2000b), "Response spectral relationships for rock sites derived from the component attenuation model", *Earthq. Eng. Struct. Dyn.*, **29**(10), 1457-1490.
Lam, N.T.K., Wilson, J.L., Chandler, A.M. and Hutchinson, G.L. (2000c), "Response spectrum modelling for rock sites in low and moderate seismicity regions combining velocity, displacement and acceleration predictions", *Earthq. Eng. Struct. Dyn.*, **29**(10), 1491-1526.
Lam, N.T.K., Wilson, J.L. and Chandler, A.M. (2001), "Seismic displacement response spectrum estimated from the frame analogy soil amplification model", *J. Eng. Struct.*, **23**, 1437-1452.
Lee, P.K.K., Kwan, A.K.H. and Zheng, W. (2000), "Tensile strength and elastic modulus of typical concrete made in Hong Kong", *Transactions of Hong Kong Institution of Engineers*, **7**(2), 35-40.
Mander, J.B., Priestley, M.J.N and Park, R. (1988), "Theoretical stress-strain model for confined concrete", *J. Struct. Eng.*, ASCE, **114**(8), 1804-1826.
Mayes, R. (1995), "Interstory drift design and damage control issues", *Journal of the Structural Design of Tall Building*, **4**, 15-25.
Mwafy, A.M. and Elnashai, A.S. (2001), "Static pushover versus dynamic collapse analysis of RC buildings", *J. Eng. Struct.*, **23**(5), 407-424.
Newmark, N.M. and Hall, W.J. (1982), *Earthquake Spectra and Design*, EERI Monograph, Earthquake Engineering Research Institute, California, USA.
Park, R. (1996), "A static force-based procedure for the seismic assessment of existing R/C moment resisting frames", *Proc. the 1996 Technical Conference of the New Zealand National Society for Earthquake Engineering*, Plymouth, 22-24 March, 54-67.
Paulay, T. and Priestey, M.J.N. (1992), *Seismic Design of Reinforced Concrete and Masonry Buildings*, John Wiley & Sons, New York.
Priestley, M.J.N. (1996), "Direct displacement seismic assessment of existing reinforced concrete buildings", *Bulletin of the New Zealand National Society for Earthquake Engineering*., **29**(4), 256-272.
Priestley, M.J.N. (1998), "Brief comments on elastic flexibility of reinforced concrete frames and significance of seismic design", *Bulletin of the New Zealand National Society for Earthquake Engineering*, **31**(4), 246-259.
Priestley, M.J.N. and Calvi, G.M. (1997), "Concepts and procedures for direct displacement-based design and assessment", *Proc. the Workshop on Seismic Design Approaches for the 21st Century*, June 1997, Slovenia.
Priestley, M.J.N. and Kowalsky, M.J. (1998), "Aspects of drift and ductility capacity of rectangular cantilever structural walls", *Bulletin of the New Zealand National Society for Earthquake Engineering*, **31**(2), 73-85.
Priestley, M.J.N. and Kowalsky, M.J. (2000), "Direct displacement-based seismic design of concrete buildings", *Bulletin of the New Zealand National Society for Earthquake Engineering*, **33**(4), 421-444.
Pun, W.K. (1994). "Earthquake resistance of buildings in Hong Kong", *Asia Engineer*, 25-28.
Scott, D.M., Pappin, J.W. and Kwok, M.K.Y. (1994), "Seismic design of buildings in Hong Kong", *Transactions of the Hong Kong Institution of Engineers.* **1**(2), 37-50.
Sheikh, N. (2001), *Simplified Analysis of Earthquake Site Response with Particular Application to Low and Moderate Seismicity Regions, MPhil Thesis*, The University of Hong Kong.
Uniform Building Code, UBC (1997), *International Conference of Building Officials*. Chapter 23, Part 3: Earthquake Design.
Waekava, K. and Xu, A. (2000), "Shear failure and ductility of RC columns after yielding of main reinforcement", *Engineering Fracture Mechanics*, **65**(2-3), Jan., 335-368.
Watson, S., Zahn, F.A. and Park, R. (1994), "Confining reinforcement for concrete columns", *J. Struct. Eng.*, ASCE, **120**(6), 1798-1824.